Arch. Mech., 44, 2, pp. 231–241, Warszawa 1992

Dynamic stress intensity factors around a rectangular crack in an elastic layer sandwiched between two elastic half-spaces

S. ITOU (YOKOHAMA)

TRANSIENT dynamic stresses around a rectangular crack in an infinite elastic layer sandwiched between two elastic half-spaces are determined. The rectangular crack is situated at the central plane of the layer, and an internal pressure is applied suddenly to its surfaces. Application of the Laplace and Fourier transforms reduces the problem to the solution of a pair of dual integral equations. To solve these equations, the Laplace transformed crack surface displacement is expanded in a double series of functions which are zero outside the crack. The unknown coefficients occurring in that series are solved with the aid of the Schmidt method. Numerical calculations are carried out for the dynamic stress intensity factors.

1. Introduction

COMPOSITE MATERIALS, such as glass fiber reinforced plastics and stainless steel fiber reinforced aluminum, have been widely used in designing the various members of machines or structures because of their many superior qualities. If we find a crack in the fiber or in the matrix, we must judge carefully whether the stress intensity factors happen to exceed the fracture toughness value of the material or not. For this purpose, it is one of the significant matters to reveal the stress intensity factors for a crack in layered media.

Many problems with regard to a crack in the composite materials are solved by Sih and his coauthors. They investigated not only the static problems but also the dynamic ones, and these works are presented in a book by SIH and CHEN [1]. In the same book, the past and present studies concerned with the cracked composite materials have been also reviewed.

As pointed by KASSIR [2], analytical solutions have been developed to treat basic geometries like those of the circular, elliptical and half-plane cracks. To overcome this point, Kassir studied the three-dimensional elastostatic problems of a rectangular crack embedded in an infinite elastic medium [2, 3]. He employed two-dimensional Fourier transforms and reduced the mixed boundary value conditions on the crack to the solution of a Fredholm integral equation of the second kind. By a somewhat different approach, the present author studied the dynamic problems of the rectangular crack(s) [4, 5, 6].

If an embedded crack is considered in the composite materials, we usually try to replace it by the penny-shaped crack and we determine the approximate values of the stress intensity factors. If the shape of the crack is rectangular rather than circular, the penny-shaped crack approach fails to be reasonable. In this case, the solutions of the stress intensity factors for a rectangular crack are needed.

In the present paper, the transient dynamic stress filed around a rectangular crack in an infinite elastic layer sandwiched between two elastic half-spaces is considered. The corresponding two-dimensional problem has been solved by SIH and CHEN [7]. The crack is placed in the mid-plane of the layer and is subjected to impact load. Following the Sih and Chen's manner, we apply the Laplace and Fourier transforms to solve the problem.

Using this technique, we can reduce the boundary conditions to dual integral equations in the Laplace transform domain. Then, the Laplace transformed crack surface displacement is expanded into double infinite series as a product of trigonometric functions. By doing so, the dual integral equations can be converted into the single integral equation in the rectangular region. The unknown coefficients accompanied in that series are solved by the Schmidt method [8]. The stress intensity factors are defined in the Laplace transform domain and these are inverted numerically in the physical plane by the method developed by MILLER and GUY [9].

2. Fundamental equations

The infinite layer is sandwiched between two half-spaces as shown in Fig. 1.

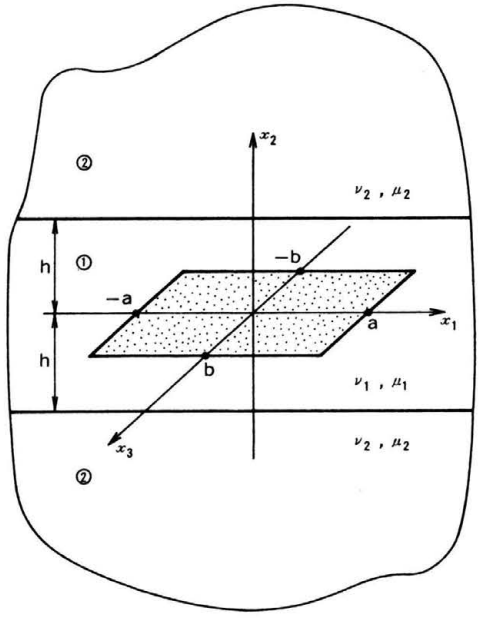

FIG. 1. Geometry and coordinate system.

The rectangular crack is located on $x_2 = 0$ along the x_1-axis from $-a$ to a, and along the x_3-axis from $-b$ to b with reference to the rectangular coordinate system (x_1, x_2, x_3). The layer and the two half-spaces are bounded at $x_2 = \pm h$. The equation of motion is

$$(\lambda_{(l)} + \mu_{(l)})u_{j(l),ji} + \mu_{(l)}u_{i(l),jj} = \rho_{(l)}\partial^2 u_{i(l)}/\partial t^2 , \tag{2.1}$$

where $u_{i(l)}$ are the displacement components, $\lambda_{(l)}$ and $\mu_{(l)}$ are the Lamé's elastic constants, $\rho_{(l)}$ is the mass density, t is time, repeated indices indicate a summation, the indices following a comma indicate the partial differentiation with respect to the variable, e.g. $u_{i(l),j} = \partial u_{i(l)}/\partial x_j$, and $(l) = (1)$ and $(l) = (2)$ are referring to the layer and the half-spaces, respectively. The stresses are expressed by the form

$$\tau_{ij(l)} = \lambda_{(l)}u_{k(l),k}\delta_{ij} + \mu_{(l)}(u_{i(l),j} + u_{j(l),i}) , \tag{2.2}$$

where δ_{ij} is the Kronecker delta.

The incident stress wave which propagates through the upper half-space can be expressed in the form

$$\tau_{22②} = p\,H(x_2 + c_{1②}t)\,, \tag{2.3}$$

where p is a constant, $c_{1①}$ is the dilatational wave velocity, and $H(t)$ is the Heaviside unit step function. If the incident wave impinges, it is reflected and refracted at the interface $x_2 = +h$, at the crack surfaces and at the interface $x_2 = -h$. However, it is very likely that a stress wave which is similar to Eq.(2.3) passes across the crack. Therefore, the boundary conditions for the problem to be studied are assumed as follows:

(2.4)

$$\begin{aligned}
&\tau^0_{22①} = -pH(t) && \text{at} \quad x_2 = 0\,, \quad |x_1| < a\,, \quad |x_3| < b\,,\\
&u^0_{2①} = 0 && \text{at} \quad x_2 = 0\,, \quad (|x_1| < a\,, b < |x_3|)\,, \quad (a < |x_1|\,, |x_3| < \infty)\,,\\
&\tau^0_{12①} = \tau^0_{23①} = 0 && \text{at} \quad x_2 = 0\,, \quad |x_1| < \infty\,, \quad |x_3| < \infty\,;
\end{aligned}$$

(2.5)

$$\begin{aligned}
&\tau_{22①} = \tau_{22②}\,, \quad \tau_{12①} = \tau_{12②}\,, \quad \tau_{23①} = \tau_{23②}\,, \quad u_{2①} = u_{2②}\,, \quad u_{1①} = u_{1②}\,,\\
&u_{3①} = u_{3②} \quad \text{at} \quad x_2 = \pm h\,, \quad |x_1| < \infty\,, \quad |x_3| < \infty\,,
\end{aligned}$$

where superscript " ^{0}" denotes the values at $x_2 = 0$. Because of the symmetry conditions, it is possible to consider the problem for $x_2 \geq 0$, only.

3. Analysis

A Laplace transform pair is defined by the equations

$$f^*(s) = \int_0^\infty f(t)\exp(-st)dt\,, \tag{3.1}$$

$$f(t) = 1/(2\pi i)\int_{\mathrm{Br}} f^*(s)\exp(st)ds\,, \tag{3.2}$$

where the second integral is over the Bromwich path. The two-dimensional Fourier transform pair is defined by the equations

$$\bar{\bar{f}}(\xi, x_2, \zeta) = \int_{-\infty}^{\infty}\int_{-\infty}^{\infty} f(x_1, x_2, x_3)\exp\{i(\xi x_1 + \zeta x_3)\}\,dx_1 dx_3\,, \tag{3.3}$$

$$f(x_1, x_2, x_3) = 1/(2\pi)^2 \int_{-\infty}^{\infty}\int_{-\infty}^{\infty} \bar{\bar{f}}(\xi, x_2, \zeta)\exp\{-i(\xi x_1 + \zeta x_3)\}\,d\xi d\zeta\,. \tag{3.4}$$

The Laplace transformed expressions of the boundary conditions (2.4) and (2.5) are

(3.5)

$$\begin{aligned}
&1)\quad \tau^{0*}_{22①} = -p/s && \text{at} \quad x_2 = 0\,, \quad |x_1| < a\,, \quad |x_3| < b\,,\\
&2)\quad u^{0*}_{2①} = 0 && \text{at} \quad x_2 = 0\,, \quad (|x_1| < a\,, b < |x_3|)\,, \quad (a < |x_1|\,, |x_3| < \infty)\,,\\
&3)\quad \tau^{0*}_{12①} = \tau^{0*}_{23①} = 0 && \text{at} \quad x_2 = 0\,, \quad |x_1| < \infty\,, \quad |x_3| < \infty\,;
\end{aligned}$$

$$\tau^*_{22①} = \tau^*_{22②}, \quad \tau^*_{12①} = \tau^*_{12②}, \quad \tau^*_{23①} = \tau^*_{23②},$$
$$\text{at} \quad x_2 = \pm h, \quad |x_1| < \infty, \quad |x_3| < \infty, \tag{3.6}$$

$$u^*_{2①} = u^*_{2②}, \quad u^*_{1①} = u^*_{1②}, \quad u^*_{3①} = u^*_{3②},$$
$$\text{at} \quad x_2 = \pm h, \quad |x_1| < \infty, \quad |x_3| < \infty,$$

Applying Eqs.(3.1) and (3.3) to Eq.(2.1) yields

$$(d^2/dx_2^2 - n^2_{1①})(d^2/dx_2^2 - n^2_{2①})u^*_{i①} = 0 \tag{3.7}$$

with

$$n_{1①} = \left\{\xi^2 + \zeta^2 + s^2/(c^2_{2①}\alpha^2_{①})\right\}^{\frac{1}{2}}, \quad n_{2①} = (\xi^2 + \zeta^2 + s^2/c^2_{2①})^{\frac{1}{2}} \tag{3.8}$$

and

$$\alpha^2_{①} = (\lambda_{①} + 2\mu_{①})/\mu_{①} = 2(1 - \nu_{①})/(1 - 2\nu_{①}), \tag{3.9}$$

where $c_{2①}$ is the shear wave velocity and $\nu_{①}$ is the Poisson's ratio. The solution of Eq.(3.7) appropriate to $x_2 \geq 0$ will take the following forms for the layer ①,

$$\begin{aligned}
\bar{u}^*_{1①} &= -i\xi A^{①}_2/n_{1①}\cosh(n_{1①}y) + B^{①}_1\cosh(n_{2①}y) \\
&\quad - i\xi C^{①}_2/n_{1①}\sinh(n_{1①}y) + D^{①}_1\sinh(n_{2①}y), \\
\bar{u}^*_{2①} &= A^{①}_2\sinh(n_{1①}y) + i(\xi B^{①}_1 + \zeta B^{①}_3)/n_{2①}\sinh(n_{2①}y) \\
&\quad + C^{①}_2\cosh(n_{1①}y) + i(\xi D^{①}_1 + \zeta D^{①}_3)/n_{2①}\cosh(n_{2①}y), \\
\bar{u}^*_{3①} &= -i\zeta A^{①}_2/n_{1①}\cosh(n_{1①}y) + B^{①}_3\cosh(n_{2①}y) \\
&\quad - i\zeta C^{①}_2/n_{1①}\sinh(n_{1①}y) + D^{①}_3\sinh(n_{2①}y),
\end{aligned} \tag{3.10}$$

and for the upper half-space②.

$$\begin{aligned}
\bar{u}^*_{1②} &= i\xi/n_{1②}A^{②}_2\exp(-n_{1②}y) + B^{②}_1\exp(-n_{2②}y), \\
\bar{u}^*_{2②} &= A^{②}_2\exp(-n_{1②}y) - i/n_{2②}(\xi B^{②}_1 + \zeta B^{②}_3)\exp(-n_{2②}y), \\
\bar{u}^*_{3②} &= i\zeta/n_{1②}A^{②}_2\exp(-n_{1②}y) + B^{②}_3\exp(-n_{2③}y),
\end{aligned} \tag{3.11}$$

where $A^{①}_2$, $B^{①}_1$, $B^{①}_3$, $C^{①}_2$, $D^{①}_1$, $D^{①}_3$, $A^{②}_2$, $B^{②}_1$, $B^{②}_3$ are the unknown coefficients to be determined from the boundary conditions.

Using Eqs.(3.10) and (3.11), we obtain the Laplace and Fourier transformed stress components. With the use of Eqs.$(3.5)_3$ and (3.6) $iB^{①}_1$, $iB^{①}_3$, $C^{①}_2$, $iD^{①}_1$, $iD^{①}_3$, $A^{②}_2$, $iB^{②}_1$ and $iB^{②}_3$ can be expressed by the single unknown $A^{①}_2$ as

$$\begin{aligned}
&iB^{①}_1 = f_1A^{①}_2, \quad iB^{①}_3 = f_2A^{①}_2, \quad C^{①}_2 = f_3A^{①}_2, \quad iD^{①}_1 = f_4A^{①}_2, \\
&iD^{①}_3 = f_5A^{①}_2, \quad A^{②}_2 = f_6A^{①}_2, \quad iB^{②}_1 = f_7A^{①}_2, \quad iB^{②}_3 = f_8A^{①}_2,
\end{aligned} \tag{3.12}$$

where $f_1, f_2, \ldots, f_8$ are shown in the Appendix.

Thus, the Laplace and Fourier transformed expressions for the stress and displacement components which satisfy Eqs.(3.5)$_3$ and (3.6) are shown with the single unknown coefficient $A_2^{①}$. For example, $\bar{\tau}_{22①}^{0*}$ and $\bar{u}_{2①}^{0*}$ have the forms

$$\begin{aligned}\bar{\tau}_{22①}^{0*} &= A_2^{①}\left[\mu_① [\{s^2/c_{2①}^2 \cdot (1-2/\alpha_{①}^2) + 2n_{1①}^2\}/n_{1①} + 2\xi f_1 + 2\zeta f_2]\right], \\ \bar{u}_{2①}^{0*} &= A_2^{①}\{f_3 + (\xi f_4 + \zeta f_5)/n_{2①}\}.\end{aligned} \tag{3.13}$$

Then the remaining boundary conditions (3.5.1) and (3.5.2) reduce to the dual integral equations

$$\text{1)} \quad \bar{\tau}_{22①}^{0*} = 1/(2\pi)^2 \int_{-\infty}^{\infty}\int_{-\infty}^{\infty} \bar{u}_{2①}^{0*} K(\xi,\zeta)\exp\{-i(\xi x_1 + \zeta x_3)\}\, d\xi d\zeta = -p/s$$

$$\text{for} \quad |x_1| < a, \quad |x_3| < b, \tag{3.14}$$

$$\text{2)} \quad \bar{u}_{2①}^{0*} = 1/(2\pi)^2 \int_{-\infty}^{\infty}\int_{-\infty}^{\infty} \bar{u}_{2①}^{0*} \exp\{-i(\xi x_1 + \zeta x_3)\}\, d\xi d\zeta = 0$$

$$\text{for} \quad (|x_1| < a, \quad b < |x_3|), \quad (a < |x_1|, \ |x_3| < \infty)$$

with

$$K(\xi,\zeta) = \mu_① \left[[\{s^2/c_{2①}^2 \cdot (1-2/\alpha_{①}^2) + 2n_{1①}^2\}/n_{1①} + 2\xi f_1 + 2\zeta f_2]/\{f_3 + (\xi f_4 + \zeta f_5)/n_{2②}\}\right]. \tag{3.15}$$

If the Laplace transformed crack surface displacement $u_{2①}^{0*}$ is expanded into the following series

$$\begin{aligned}\pi^2 u_{2①}^{0*} &= \sum_{m=1}^{\infty}\sum_{n=1}^{\infty} c_{mn}(s) \cdot \cos\{(2m-1)\sin^{-1}(x_1/a)\} \\ &\quad \times \cos\{(2n-1)\sin^{-1}(x_3/b)\} \quad \text{for} \quad |x_1| < a, \quad |x_3| < b, \\ \pi^2 u_{2①}^{0*} &= 0 \quad \text{for} \quad (|x_1| < a, \ b < |x_3|), \quad (a < |x_1|, \ |x_3| < \infty)\end{aligned} \tag{3.16}$$

the boundary condition (3.14)$_2$ is satisfied automatically, where $c_{mn}(s)$ are unknown coefficients to be determined. The Fourier transformation of Eq. (3.16) is

$$\bar{u}_{2①}^{0*} = \sum_{m=1}^{\infty}\sum_{n=1}^{\infty} c_{mn}(s)(2m-1)/\xi \cdot J_{2m-1}(\xi a) \cdot (2n-1)/\zeta \cdot J_{2n-1}(\zeta b), \tag{3.17}$$

where $J_n(x)$ is the Bessel function. Substituting Eq.(3.17) into Eq.(3.14)$_1$, we obtain the following equation which gives the unknown coefficients $c_{mn}(s)$

$$\begin{aligned}\sum_{m=1}^{\infty}\sum_{n=1}^{\infty} c_{mn}(s)[(2m-1)(2n-1) \int_0^{\infty}\int_0^{\infty} K(\xi,\zeta)/(\xi^2\zeta^2) J_{2m-1}(\xi a) J_{2n-1}(\zeta b) \\ \times \sin(\xi x_1)\sin(\zeta x_3) d\xi d\zeta] = -p x_1 x_3/s \\ \text{for} \quad 0 \le x_1 < a, \quad 0 \le x_3 < b.\end{aligned} \tag{3.18}$$

The semi-infinite integral in Eq.(3.18) is replaced in the same manner as in the author's previous paper [4] to achieve rapid decay when ξ and ζ become large

$$(3.19)\quad \int_0^\infty \int_0^\infty d\xi d\zeta = \int_0^\infty \{g_m(x_1,\zeta) - g_m(x_1,\zeta_l)\zeta/\zeta_l\}/\zeta^2 \cdot J_{2n-1}(\zeta b)\sin(\zeta x_3)d\zeta + g_m(x_1,\zeta_l)/\{\zeta_l(2n-1)\}\sin\{(2n-1)\sin^{-1}(x_3/b)\}$$

with

$$(3.20)\quad g_m(x_1,\zeta) = \int_0^\infty \{K(\xi,\zeta)/\xi - K(\xi_l,\zeta)/\xi_l\} \cdot J_{2m-1}(\xi a)\sin(\xi x_1)d\xi + K(\xi_l,\zeta)/\{\xi_l(2m-1)\} \cdot \sin\{(2m-1)\sin^{-1}(x_1/a)\},$$

where ξ_l and ζ_l are large values of ξ and ζ, respectively, and $\xi \gg \zeta$ is assumed for the large value of ξ. The integrands in Eq.(3.19) and that in Eq.(3.20) behave as $\zeta^{-2.5}$ and $\xi^{-2.5}$ for large ζ and ξ, respectively. Therefore, those semi-infinite integrals can be easily evaluated numerically by the Filon's method [10]. Then, Eq.(3.18) can be solved for the coefficients $c_{mn}(s)$ by the Schmidt method [8].

4. Stress intensity factors

The coefficients $c_{mn}(s)$ are obtainable, so that the entire stress field is given. However, in fracture mechanics, it is of importance to determine stresses just ahead of the crack end. The stress singularities around the crack tip come from the behavior of the integrand as the integration variable has an infinite value. Therefore, we can easily define the stress intensity factors K_I^{b*} along $x_3 = b$ and K_I^{a*} along $x_1 = a$ as, respectively,

$$(4.1)\quad K_I^{b*} = \sqrt{2\pi(x_3-b)}\tau_{22①}^{0*}|_{x_3\to b+} = \sum_{m=1}^\infty \sum_{n=1}^\infty c_{mn}(s)(2n-1)(-1)^n\sqrt{\pi/b}K(\xi,\zeta_l)/\zeta_l \times \cos\{(2m-1)\sin^{-1}(x_1/a)\},$$

$$K_I^{a*} = \sqrt{2\pi(x_1-a)}\tau_{22①}^{0*}|_{x_1\to a+} = \sum_{m=1}^\infty \sum_{n=1}^\infty c_{mn}(s)(2n-1)(-1)^m\sqrt{\pi/a}K(\xi_l,\zeta)/\xi_l \times \cos\{(2n-1)\sin^{-1}(x_3/b)\}.$$

The inverse Laplace transformations in Eq.(4.1) are carried out by the numerical method given by MILLER and GUY [9]. When the Laplace transform $f^*(s)$ can be evaluated at discrete points given by

$$(4.2)\quad s = (\beta + 1 + k), \quad k = 0,1,2,\ldots,$$

we determine coefficients C_m from the following set of equations

$$(4.3)\quad \delta' f^*\{(\beta+1+k)\delta'\} = \sum_{m=0}^k C_m k!/\{(k+\beta+1)(k+\beta+2)\ldots(k+\beta+1+m)(k-m)!\},$$

where $\delta' > 0$ and $\beta > -1$. If coefficients are calculated up to C_{N-1}, an approximate value of $f(t)$ can be found as

$$(4.4)\quad f(t) = \sum_{m=0}^{N-1} C_m P_m^{(0,\beta)}\{2\exp(\delta' t) - 1\},$$

where $P_m^{(\alpha,\beta)}(z)$ is the Jacobi polynomial. The parameters δ' and β are selected such that $f(t)$ can be best described within a particular range of time t.

We have the relation between $f^*(s)$ and $f(t)$,

$$\lim_{s\to 0} s \cdot f^*(s) = \lim_{t\to\infty} f(t). \tag{4.5}$$

Therefore, the static solutions of the stress intensity factors in the physical space can be obtained with the use of Eqs.(4.1) and (4.5).

5. Numerical examples and results

The transient dynamic stress intensity factors are calculated numerically for $\nu_① = \nu_② = 0.2$. It is assumed that the density of the layer is equal to those of the half-spaces. The semi-infinite integrals which occur in Eqs.(3.19) and (3.20) can be easily evaluated numerically by Filon's method. In Table 1, the values of $K(\xi b, \zeta b)/(\xi b)$ are shown versus ξb for $sb/c_{2①} = 2.2$, $\mu_②/\mu_① = 0.5$, $a/b = 1.0$ and $h/b = 1.0$. In Table 2, the values of $g_m(x_1/b, \zeta b)/(\zeta b)$ are also shown versus ζb for $sb/c_{2①} = 2.2$, $\mu_②/\mu_① = 0.5$, $a/b = 1.0$, $h/b = 1.0$, $m = 2$ and $x_1/b = 0.5$. The values of $K(\xi b, \zeta b)/(\xi b)$ and $g_m(x_1/b, \zeta b)/(\zeta b)$ converge at constant values and then we can see that the numerical integrations can be carried out satisfactorily.

Table 1. Values of $K(\xi b, \zeta b)/(\xi b)$ for $sb/c_{2①} = 2.2$, $\mu_②/\mu_① = 0.5$, $a/b = 1.0$, $h/b = 1.0$.

	$K(\xi b, \zeta b)/(\xi b)$			
ξb	$\zeta b = 3.21$	6.81	10.41	14.01
⋮	⋮	⋮	⋮	⋮
78.21	−1.2516	−1.2567	−1.2638	−1.2719
78.41	−1.2514	−1.2565	−1.2633	−1.2708
78.61	−1.2513	−1.2564	−1.2628	−1.2700
78.81	−1.2513	−1.2563	−1.2625	−1.2693
79.01	−1.2512	−1.2561	−1.2621	−1.2686
⋮	⋮	⋮	⋮	⋮
97.21	−1.2510	−1.2550	−1.2612	−1.2629
97.41	−1.2510	−1.2549	−1.2609	−1.2625
97.61	−1.2510	−1.2549	−1.2606	−1.2621
97.81	−1.2510	−1.2548	−1.2605	−1.2617
98.01	−1.2510	−1.2547	−1.2603	−1.2613

By breaking-off the infinite series in Eq.(3.18) at term of $m = n = 4$ the Schmidt method is applied. Table 3 shows the values at the right-hand and the left-hand side of Eq.(3.18) in the case of $sb/c_{2①} = 2.2$, $\mu_②/\mu_① = 0.5$, $a/b = 1.0$ and $h/b = 1.0$. The upper side values are $1/(pb^3/c_{2①}) \cdot \sum_{m=1}^{4}\sum_{n=1}^{4} c_{mn}(s)[(2m-1)(2n-1)\int_0^\infty\int_0^\infty K(\xi,\zeta)/(\xi^2\zeta^2)$ $J_{2m-1}(\xi a)J_{2n-1}(\zeta b)\sin(\xi x_1)\sin(\zeta x_3)d\xi d\zeta$ and the lower side values with parenthesis are $-(x_1x_3)/(sb^3/c_{2①})$. Both values of these coincide mutually well, thus it is considered that precision of the Schmidt method is superior.

Table 2. Values of $g_m(x_1/b, \zeta b)/(\zeta b)$ for $sb/c_{2①} = 2.2$, $\mu_②/\mu_① = 0.5$, $a/b = 1.0$, $h/b = 1.0$, $x_1/b = 0.5$, $m = 2$.

ζb	$g_m(x_1/b, \zeta b)/(\zeta b)$
⋮	⋮
6.01	−0.16575
6.21	−0.16400
6.41	−0.16239
6.61	−0.16091
6.81	−0.15954
7.01	−0.15712
⋮	⋮
13.01	−0.14238
13.21	−0.14217
13.41	−0.14197
13.61	−0.14178
13.81	−0.14160
14.01	−0.14143

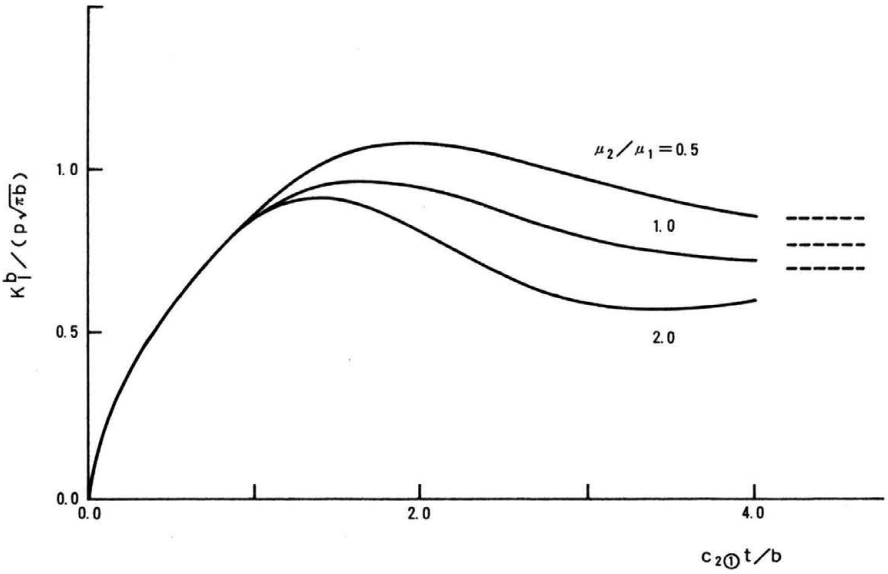

FIG. 2. Stress intensity factor K_I^b at $x_1/a = 0.0$ for $a/b = 1.0$ and $h/b = 1.0$.

In Fig. 2, the values of K_I^b at $x_1/a = 0.0$ are plotted versus $c_{2①}t/b$ for $\mu_②/\mu_① = 0.5$, 1.0, 2.0 in the case of $h/b = 1.0$, $a/b = 1.0$. The corresponding static values which are calculated by means of Eq.(4.5) are also drawn by the straight broken lines in the figure. From the figure, we can see that the peak value K_I^b for $\mu_②/\mu_① = 0.5$ is about 1.1 times larger than that for $\mu_②/\mu_① = 1.0$ while the peak value for $\mu_②/\mu_① = 2.0$ shows a decrease of 5% in comparison with the value for $\mu_②/\mu_① = 1.0$. It can be also seen that the peak values of the dynamic stress intensity factors are about 1.25 or 1.30 larger than the corresponding static values.

Table 3. Values of $1/(pb^3/c_{2①}) \cdot \sum_{m=1}^{4}\sum_{n=1}^{4} c_{mn}(s)[(2m-1)(2n-1) \times \int_0^\infty \int_0^\infty K(\xi,\zeta)/(\xi^2\zeta^2) J_{2m-1}(\xi a) J_{2n-1}(\zeta b) \times \sin(\xi x_1)\sin(\zeta x_3) d\xi d\zeta$ **and** $-(x_1x_3)/(sb^3/c_{2①})$ **for** $sb/c_{2①} = 2.2$, $\mu_②/\mu_① = 0.5$, $a/b = 1.0$, $h/b = 1.0$.

	$x_1/b = 0.0$	0.25	0.5	0.75	1.0
$x_3/b = 0.0$	0.0 (0.0)	0.0 (0.0)	0.0 (0.0)	0.0 (0.0)	0.0 (0.0)
0.25	0.0 (0.0)	−0.02842 (−0.02841)	−0.05683 (−0.05682)	−0.08525 (−0.08523)	−0.11368 (−0.11364)
0.50	0.0 (0.0)	−0.05681 (−0.05682)	−0.11361 (−0.11364)	−0.12783 (−0.12784)	−0.22719 (−0.22727)
0.75	0.0 (0.0)	−0.08525 (−0.08523)	−0.17048 (−0.17045)	−0.25575 (−0.25568)	−0.34102 (−0.34091)
1.0	0.0 (0.0)	−0.11363 (−0.11364)	−0.22729 (−0.22727)	−0.34091 (−0.34091)	−0.45457 (−0.45454)

Appendix

$$\text{(A.1)}\qquad f_i = \begin{vmatrix} a_{11} & \cdots & a_{1i-1} & b_1 & a_{1i+1} & \cdots & a_{18} \\ a_{21} & \cdots & a_{2i-1} & b_2 & a_{2i+1} & \cdots & a_{28} \\ \vdots & & \vdots & \vdots & \vdots & & \vdots \\ a_{71} & \cdots & a_{7i-1} & b_7 & a_{7i+1} & \cdots & a_{78} \\ a_{81} & \cdots & a_{8i-1} & b_8 & a_{8i+1} & \cdots & a_{88} \end{vmatrix} / D,$$

$$\text{(A.2)}\qquad D = |a_{ij}|$$

and

$$\begin{aligned}
&a_{11} = 0, \quad a_{12} = 0, \quad a_{13} = 2\xi, \quad a_{14} = (n_{2①}^2 + \xi^2)/n_{2①}, \quad a_{15} = \xi\zeta/n_{2①}, \\
&a_{16} = 0, \quad a_{17} = 0, \quad a_{18} = 0, \quad b_1 = 0, \\
&a_{21} = 0, \quad a_{22} = 0, \quad a_{23} = 2\zeta, \quad a_{24} = \xi\zeta/n_{2①}, \quad a_{25} = (n_{2①}^2 + \zeta^2)/n_{2①}, \\
&a_{26} = 0, \quad a_{27} = 0, \quad a_{28} = 0, \quad b_2 = 0, \\
&a_{31} = 2\xi\mu_① \cosh(n_{2①}h), \quad a_{32} = 2\zeta\mu_① \cosh(n_{2①}h), \\
&a_{33} = \{s^2/c_{2①}^2 \cdot (1 - 2/\alpha_{①}^2) + 2n_{1①}^2\}/n_{1①} \cdot \mu_① \sinh(n_{1①}h), \\
&a_{34} = 2\xi\mu_① \sinh(n_{2①}h), \quad a_{35} = 2\zeta\mu_① \sinh(n_{2①}h), \\
&a_{36} = \{s^2/c_{2②}^2 \cdot (1 - 2/\alpha_{②}^2) + 2n_{1②}^2\}/n_{1②} \cdot \mu_② \exp(-n_{1②}h), \\
&a_{37} = -2\xi\mu_② \exp(-n_{2②}h), \quad a_{38} = -2\zeta\mu_② \exp(-n_{2②}h), \\
&b_3 = -\{s^2/c_{2①}^2 \cdot (1 - 2/\alpha_{①}^2) + 2n_{1①}^2\}/n_{1①} \cdot \mu_① \cosh(n_{1①}h), \\
&a_{41} = (n_{2①}^2 + \xi^2)/n_{2①} \cdot \mu_① \sinh(n_{2①}h), \quad a_{42} = \xi\zeta/n_{2①} \cdot \mu_① \sinh(n_{2①}h), \\
&a_{43} = 2\xi\mu_① \cosh(n_{1①}h), \quad a_{44} = (n_{2①}^2 + \xi^2)/n_{2①} \cdot \mu_① \cosh(n_{2①}h), \\
&a_{45} = \xi\zeta/n_{2①} \cdot \mu_① \cosh(n_{2①}h), \quad a_{46} = -2\xi\mu_② \exp(-n_{1②}h), \\
&a_{47} = (n_{2②}^2 + \xi^2)/n_{2②} \cdot \mu_② \exp(-n_{2②}h), \quad a_{48} = \xi\zeta/n_{2②} \cdot \mu_② \exp(-n_{2②}h), \\
&b_4 = -2\xi\mu_① \sinh(n_{1①}h), \qquad \text{(A.3)} \\
&a_{51} = \xi\zeta/n_{2①} \cdot \mu_① \sinh(n_{2①}h), \quad a_{52} = (n_{2①}^2 + \zeta^2)/n_{2①} \cdot \mu_① \sinh(n_{2①}h), \\
&a_{53} = 2\zeta\mu_① \cosh(n_{2①}h), \quad a_{54} = \xi\zeta/n_{2①} \cdot \mu_① \cosh(n_{2①}h), \\
&a_{55} = (n_{2①}^2 + \zeta^2)/n_{2①} \cdot \mu_① \cosh(n_{2①}h), \quad a_{56} = -2\zeta\mu_② \exp(-n_{1②}h), \\
&a_{57} = \xi\zeta/n_{2②} \cdot \mu_② \exp(-n_{2②}h), \quad a_{58} = (n_{2②}^2 + \zeta^2)/n_{2②} \cdot \mu_② \exp(-n_{2②}h), \\
&b_5 = -2\zeta\mu_① \sinh(n_{1①}h), \\
&a_{61} = \xi/n_{2①} \sinh(n_{2①}h), \quad a_{62} = \zeta/n_{2①} \sinh(n_{2①}h), \quad a_{63} = \cosh(n_{1①}h), \\
&a_{64} = \xi/n_{2①} \cosh(n_{2①}h), \quad a_{65} = \zeta/n_{2①} \cosh(n_{2①}h), \\
&a_{66} = -\exp(-n_{1②}h),
\end{aligned}$$

$$a_{67} = \xi/n_{2②} \exp(-n_{2②}h), \quad a_{68} = \zeta/n_{2②} \exp(-n_{2②}h),$$
$$b_6 = -\sinh(n_{1①}h),$$

$$a_{71} = \cosh(n_{2①}h), \quad a_{72} = 0, \quad a_{73} = \xi/n_{1①} \cdot \sinh(n_{1①}h),$$
$$a_{74} = \sinh(n_{2①}h), \quad a_{75} = 0, \quad a_{76} = \xi/n_{1②} \cdot \exp(-n_{1②}h),$$
$$a_{77} = -\exp(-n_{2②}h), \quad a_{78} = 0, \quad b_7 = -\xi/n_{1①} \cdot \cosh(n_{1①}h),$$
$$a_{81} = 0, \quad a_{82} = \cosh(n_{2①}h), \quad a_{83} = \zeta/n_{1①} \sinh(n_{1①}h), \quad a_{84} = 0,$$
$$a_{85} = \sinh(n_{2①}h), \quad a_{86} = \zeta/n_{1②} \exp(-n_{1②}h), \quad a_{87} = 0,$$
$$a_{88} = -\exp(-n_{2②}h), \quad b_8 = -\zeta/n_{1①} \cosh(n_{1①}h).$$

References

1. G.C. SIH and E.P. CHEN *Mechanics of fracture 6. Cracks in composite materials*, M. Nijhoff Publ., Hague 1981.
2. M.K. KASSIR, *Stress-intensity factor for a three-dimensional rectangular crack*, ASME J. Appl. Mech., **48**, 309-312, 1981.
3. M.K. KASSIR, *A three-dimensional rectangular crack subjected to shear loading*, Int. J. Solids Struct., **18**, 1075-1082, 1982.
4. S. ITOU, *Dynamic stress concentration around a rectangular crack in an infinite elastic medium*, Zeitschrift für Angewandte Mathematik und Mechanik, **60**, 317-322,1980.
5. S. ITOU, *Transient analysis of stress waves around a rectangular crack under impact load*, ASME J. Appl. Mech., **47**, 958-959,1980.
6. S. ITOU, *Transient analysis of stress waves around two rectangular cracks under impact load*, Engng. Fract. Mech., **14**, 685-695, 1981.
7. G.C. SIH and E.P. CHEN, *Normal and shear impact of layered composite with a crack: dynamic stress intensification*, ASME J. Appl. Mech. **47**, 351-358, 1980.
8. P.M. MORSE and H. FESHBACH, *Methods of theoretical physics*, Mc Graw-Hill, vol. 1, 926-931, New York 1958.
9. M.K. MILLER and W.T. GUY, *Numerical inversion of the Laplace transform by use of Jacobi polynomials*, SIAM J. Num. Anal., **3**, 624-635, 1966.
10. A. AMEMIYA and T. TAGUCHI, *Numerical analysis and Fortran* [in Japanese], 186-193, Maruzen, Tokyo 1969.

DEPARTMENT OF MECHANICAL ENGINEERING
KANAGAWA UNIVERSITY, YOKOHAMA, JAPAN.

Received January 2, 1992.